COMMUNICATION

ChemComm
www.rsc.org/chemcomm

Nanostructured zeolite 4A molecular sieving air separation membranes†

Huanting Wang, Limin Huang, Brett A. Holmberg and Yushan Yan*

Department of Chemical and Environmental Engineering, University of California, Riverside, California 92521, USA. E-mail: yushan.yan@ucr.edu; Fax: +1-909-787-5696; Tel: +1-909-787-2068

Received (in Cambridge, UK) 20th May 2002, Accepted 27th June 2002
First published as an Advance Article on the web 9th July 2002

A novel membrane forming strategy is reported to probe the intrinsic O_2/N_2 selectivity of zeolite 4A membrane and to fabricate highly selective nanocomposite membranes by using a nanocrystal-derived hierarchical porous zeolite 4A membrane whose non-zeolitic mesoporsity is filled with a nonpermeable polymer material (polyfurfuryl alcohol).

Zeolite membranes have been widely studied for potentially highly selective molecular sieving gas separations. Among various gas pairs, separation of air into oxygen and nitrogen is an important one and is currently achieved primarily by energy-intensive cryogenic distillation.[1] Zeolite 4A has a nominal pore size of 4 Å, which falls between the molecular size of O_2 and N_2 (O_2: 3.8 Å × 2.8 Å, N_2: 4.2 Å × 3.2 Å), and therefore zeolite 4A membranes could be particularly well suited for air separation.[2–4] During the past decade, several techniques including microwave heating synthesis,[5] dry-gel conversion,[6] *in-situ* and secondary growth[7,8] have been developed for preparing pure polycrystalline zeolite 4A membranes. However, the O_2/N_2 separation factor of zeolite 4A membranes obtained so far is still below 2.0, a number too low for commercial use. There are two possible reasons for the observed low O_2/N_2 selectivity of zeolite 4A membranes: (1) existing zeolite 4A membranes are defective, *i.e.*, containing cracks, pinholes, and inter-crystal gaps; (2) zeolite 4A crystals actually do not possess high O_2/N_2 selectivity as previously predicted.[9]

To provide an answer to this challenging question, here we report a novel strategy that could potentially bypass the difficulty of preparing a defect-free pure zeolite 4A membrane. Specifically we use a zeolite A-polyfurfuryl alcohol nanocomposite membrane as the model system. The nanocomposite membrane is fabricated by using a nanocrystal-derived hierarchical porous[10,11] zeolite A membrane whose non-zeolitic mesoporsity is filled with nonpermeable polyfurfuryl alcohol. Because of the use of nanometer sized crystals, it is expected that zeolitic channels in the hierarchical porous zeolite structure remain well-connected to provide continuous zeolitic transport pathways for guest molecules. Polyfururyl alcohol (PFA) is chosen to fill inter-particle mesopores since crosslinked PFA is very dense[12,13] and can be easily deposited by using vapor deposition polymerization (VDP) from its monomer — furfuryl alcohol.[13]

Fig. 1 shows a fabrication protocol of nanocomposite membranes. Porous α-Al_2O_3 tubes with 7.4 mm OD, 6.0 mm ID, 0.15 μm mean pore diameter (Dongsuh Ltd., Korea) were dip-coated by draining zeolite A-ethanol suspension (see ESI†)[14] at around 1 cm s^{-1} through the inner surface of the tube. Zeolite A nanocrystals then self-assembled into a continuous layer on the alumina surface during drying. The tubes with a zeolite A layer were heat-treated at heating rate of 2 °C min^{-1} to 450 °C, and kept at that temperature for 6 h to burn off the structure-directing-agent (TMAOH), and also to improve binding among zeolite A nanocrystals and between zeolite A

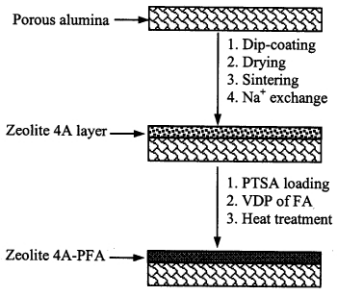

Fig. 1 Fabrication protocol of zeolite A-polyfurfuryl alcohol nanocomposite membranes by dip-coating of zeolite 4A nanocrystal suspension and vapor deposition polymerization (VDP) of furfuryl alcohol (FA).

nanocrystals and porous alumina support through condensation crosslinking of surface silanol groups of nanocrystals.[10,11] To obtain zeolite 4A (NaA) form, calcined zeolite A coated tubes were treated in 10% $NaNO_3$ aqueous solution at 80 °C for 10 h allowing for sodium ion exchange, and this was followed by washing with DI water and calcination at 450 °C for 2 h to completely remove possible residual NO_3^-.

SEM images (Fig. 2a,b) show that a zeolite A layer of 3–5 μm thick is uniformly deposited on an alumina support. The A nanocrystals are densely packed, and the average crystal size of zeolite A is about 120 nm. Zeolite nanocrystals before and after sodium exchange were examined by X-ray diffraction. Only A-type phase is found in the XRD patterns (see ESI†).

To estimate inter-crystal pore size, and to evaluate effectiveness of sodium ion exchange, Nitrogen adsorption–desorption was measured on zeolite A samples obtained under the same conditions for preparation of zeolite A layers on alumina tube (see ESI†). The calcined and sodium exchanged samples show presence of micropores and mesopores. The micropore volume

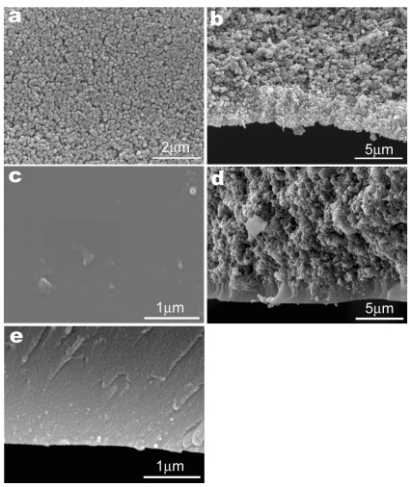

Fig. 2 SEM images of zeolite A coated porous alumina tube (a, b) and zeolite A-polyfurfuryl alcohol nanocomposite membrane (c, d, e). (a) Surface view of zeolite A layer; (b) Cross-sectional view; (c) Surface view; (d) Cross-sectional view; (e) Cross section at higher magnification.

† Electronic supplementary information (ESI) available: nanocrystal synthesis and characterization. See http://www.rsc.org/suppdata/cc/b2/b204854j/

DOI: 10.1039/b204854j

of the calcined sample is determined to be 0.30 $cm^3\ g^{-1}$, and A Brunaer–Emmett–Teller (BET) surface area is calculated to be 704 $m^2\ g^{-1}$. After sodium ion exchange, the micropore volume drops to 0.18 $cm^3\ g^{-1}$, indicating that the presence of sodium ion does reduce the window size of zeolite A frameworks. However, the micropore volume did not decrease to zero as expected for true 4A crystals possibly because the Na^+ ion exchange was incomplete or the A crystals had a Si/Al ratio higher than 1 due to the use of TMA in the synthesis.[15] Further studies are underway to clarify this. Based on nitrogen adsorption data, the mesopore volume and mesopore size of the zeolite 4A layer are estimated to be 0.25 $cm^3\ g^{-1}$ and 27 nm, respectively.

The tubes with a zeolite 4A layer were impregnated with 0.5 mol L^{-1} ethanol solution of *p*-toluene sulfonic acid (PTSA, Alfa). After drying at 90 °C for 2 h, the PTSA was located in inter-nanocrystal voids since its molecular size (>0.593 nm toluene diameter) is larger than a zeolitic pore. The tubes were then exposed to furfuryl alcohol (FA, Aldrich) vapor at 90 °C. The FA vapor penetrated into the inter-particle pores of the zeolite 4A layer, and polymerized under acid-catalysis of PTSA. It is noted that the molecular size of furfuryl alcohol ($8.43 \times 6.44 \times 4.28$ Å) is larger than zeolite A pore size, and therefore furfuryl alcohol molecules should not penetrate into zeolite A pore channels. The vapor-deposition-polymerization process took about 4 h to completely fill inter-crystal voids. SEM images show that a zeolite A–PFA nanocomposite layer has a fairly smooth surface (Fig. 2c), and a thickness of *ca.* 3 μm on an alumina support (Fig. 2d). At high magnification SEM (Fig. 2e), the nanocomposite exhibits nano-sized features composed of zeolite A nanocrystals and polyfurfuryl alcohol. In the course of VDP, some furfuryl alcohol could initially penetrate through the zeolite 4A layer, and deposit at the interface between the zeolite 4A layer and the porous alumina. However, alumina pore size is much greater than zeolite inter-particle pore (μm *vs.* nm), and thus as VDP proceeds, inter-particle porosity decreases much faster, limiting further deposition at the interface. As a result, the alumina tube remains highly permeable after the VDP process (Fig. 2d).

The VDP samples were heated at 130 °C for 120 minutes to complete polymerization and crosslinking[12,13] and the resultant zeolite 4A-PFA composite membrane is denoted as M130. M130 was directly tested for air separation. Other samples obtained were further heated at 1 °C min^{-1} to 250, 350, 400, 450 °C, respectively, and kept at the corresponding temperature for 60 min.

Fig. 3 shows air separation results of the samples measured at 30 °C. As expected, sample M130 has already shown an O_2/N_2 selectivity as high as 4.6, and an oxygen permeance of 1.5×10^{-9} mol m^{-2} s Pa. It is reported that existing pure zeolite 4A membranes have the same order of magnitude of permeance but lower selectivity.[10,11] Oxygen permeance of the samples increased from 1.5×10^{-9} to 3.4×10^{-8} mol m^{-2} s Pa when they were heat-treated from 130 to 450 °C under flowing N_2.

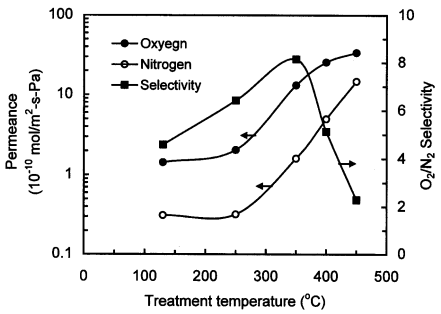

Fig. 3 O_2 and N_2 permeances and O_2/N_2 separation factors of A-PFA nanocomposite membranes under heat-treatment at different temperatures.

The sample shows a highest oxygen/nitrogen separation selectivity of 8.2 after heat-treatment at 350 °C. The O_2/N_2 selectivity of the nanocomposite membrane decreases to 2.3 when heat-treatment temperature increases up to 450 °C.

It has been reported that homogenously crosslinked PFA is very dense, and there is no detectable gas permeation through the PFA layers.[12,13] Thus the O_2/N_2 selectivity of M130 (*i.e.*, 4.6) should reflect the performance of a pure zeolite 4A membrane. However, VDP-PFA, PTSA and non-polymerized FA trapped in the composite layers may modify the pore window of zeolite A nanocrystals. Consequently, it is possible that the obtained O_2/N_2 selectivity = 4.6 is not the true selectivity of zeolite 4A. To remove this effect, the nanocomposite membranes are heat-treated to clean the pore windows of zeolite A nanocrystals. The O_2/N_2 selectivity of zeolite A-PFA nanocomposite membranes does increase with heat-treatment temperature. It should be mentioned that the structure of polyfurfuryl alcohol varies with increasing heat-treatment temperature. The furan rings in the PFA start to open above 100 °C, and benzene rings begin to form between chain fragments at around 300–350 °C (see TG analysis and elemental analysis in ESI†). PFA started to become porous at a pyrolysis temperature over 300 °C.[12,16] Contribution of heat-treated PFA to air separation through the nanocomposite membranes may be ignored since heat-treated PFA possesses extremely low gas permeation (10^{-11} mol m^{-2} s Pa).[12] More investigations are needed to fully understand the gas transport mechanism through the nanocomposite membranes.

This study suggests that the intrinsic O_2/N_2 selectivity (4.6–8.2) of zeolite 4A appears to be higher than experimentally reported on pure polycrystalline 4A membranes. It is important to note that with a true 4A membrane, it is likely that the O_2/N_2 selectivity will be much higher than the one reported here. It is believed that the technique developed here could be readily extended to other zeolite-based membranes, the combination of dip-coating and a nonpermeable filler provides a powerful tool to manufacture large-scale, high-performance zeolite-based composite membranes.

This work was supported in part by Riverside Public Utilities, California Energy Commission, US-EPA, UC-SMART, and UC-TSR&TP. We thank Professors D. H. Olson and G. H. Kuehl of University of Pennsylvania for helpful discussion.

Notes and references

1 R. T. Yang, *Gas separation by adsorption processes*, Butterworth Publications, Stoneham, MA, USA, 1987.
2 J. Izumi and M. Suzuki, *Adsorption*, 2000, **6**, 205.
3 J. Karger and D. M. Ruthven, *Diffusion in zeolites and other microporous solids*, Wiley-Interscience Publications, New York, 1992.
4 R. Mahajan and W. J. Koros, *Ind. Eng. Chem. Res.*, 2000, **39**, 2692.
5 X. C. Xu, W. S. Yang, J. Liu and L. W. Lin, *Adv. Mater.*, 2000, **12**, 195.
6 Y. H. Ma, Y. J. Zhou, R. Poladi and E. Engwall, *Sep. Purif. Technol.*, 2001, **25**, 235.
7 L. C. Boudreau, J. A. Kuck and M. Tsapatsis, *J. Membr. Sci.*, 1999, **152**, 41.
8 K. Aoki, K. Kusakabe and S. Morooka, *J. Membr. Sci.*, 1998, **141**, 197.
9 P. S. Rallabandi and D. M. Ford, *AIChE J.*, 2000, **46**, 99.
10 L. M. Huang, Z. B. Wang, J. Y. Sun, L. Miao, Q. Z. Li, Y. S. Yan and D. Y. Zhao, *J. Am. Chem. Soc.*, 2000, **122**, 3530.
11 H. T. Wang, L. M. Huang, Z. B. Wang, A. Mitra and Y. S. Yan, *Chem. Commun.*, 2001, 1364.
12 M. B. Shiflett and H. C. Foley, *Science*, 1999, **285**, 1902.
13 H. T. Wang, L. X. Zhang and G. R. Gavalas, *J. Membr. Sci.*, 2000, **177**, 25.
14 S. Mintova, N. H. Olson, V. Valtchev and T. Bein, *Science*, 1999, **283**, 958.
15 D. W. Breck, W. G. Eversole, R. M. Milton, T. B. Reed and T. L. Thomas, *J. Am. Chem. Soc.*, 1956, **78**, 5963.
16 A. Shindo and K. Izumino, *Carbon*, 1994, **32**, 1233.